Boron and Nitrogen Doping Induced Half-Metallicity in Zigzag Triwing Graphene Nanoribbons

ARTICLE *in* THE JOURNAL OF PHYSICAL CHEMISTRY C · MARCH 2011

Impact Factor: 4.77 · DOI: 10.1021/jp110649m

4 AUTHORS, INCLUDING:

Hong Hu
The Hong Kong Polytechnic University
143 PUBLICATIONS **1,105** CITATIONS
SEE PROFILE

Liyan Zhu
National University of Singapore
32 PUBLICATIONS **369** CITATIONS
SEE PROFILE

THE JOURNAL OF PHYSICAL CHEMISTRY C

ARTICLE

pubs.acs.org/JPCC

Boron and Nitrogen Doping Induced Half-Metallicity in Zigzag Triwing Graphene Nanoribbons

Liang Ma,[†] Hong Hu,[‡] Liyan Zhu,[†] and Jinlan Wang[†,§,*]

[†]Department of Physics, Southeast University, Nanjing, 211189, China

[‡]Institute of Textiles and Clothing, Hong Kong Polytechnic University, Kowloon, Hong Kong, China

[§]School of Chemistry & Chemical Engineering, Southeast University, Nanjing, 211189, China

Supporting Information

ABSTRACT: The electronic and magnetic properties of quasi-1D zigzag triwing graphene (ZZ-TWG) ribbons with boron and nitrogen (BN) doping were investigated by means of a spin-polarized density functional theory approach. Our results showed that asymmetric BN doping can give rise to half-metallicity and suppress spin polarization of the doped wings, making the BN-doped ZZ-TWGs potential application in spintronics devices. Heavily doping can turn metallic ZZ-TWG ribbons into semiconductors. A critical ratio of BN to C and appropriate doping site (e.g., ribbon's edges) are required for achieving specific electronic properties. An effective path of engineering electronic properties of ZZ-TWGs by BN doping was suggested.

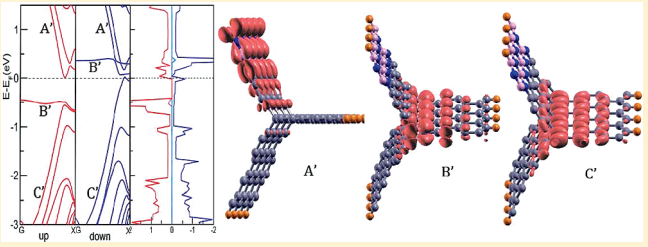

I. INTRODUCTION

Having been first synthesized experimentally in 2004,[1] graphene, the monolayer of graphite, has attracted extensively interest due to its unique electronic properties such as exceptionally high carrier mobility[2] and quantization of conductivity,[1] which arise from an unusual linear energy dispersion at Dirac points.[3−5] Because of the absence of an effective band gap in graphene, which greatly limits the possibility of application in real electronic devices,[6] quasi-1D graphene nanoribbons (GNRs) with the promise of introducing a proper gap by lateral confining were intensively investigated.[7−12] Both armchair- and zigzag-edged GNRs (labeled as AM-GNRs and ZZ-GNRs, respectively) were predicted to be semiconductors by first-principles calculations[7,8] and later were confirmed experimentally.[9,10] Besides, the band gap of AM-GNRs decreasingly oscillates as increasing of ribbon width with a periodicity of 3 (here the number of armchair chains denotes the ribbon width).[7,8] ZZ-GNRs exhibit two localized ferromagnetically ordered edge states that are antiferromagnetically coupled.[7,11,12]

Band gap is a basic property of semiconductors and insulators that essentially determines their transport properties. A tunable electronic structure would thus be highly ideal for flexibly designing semiconductor devices. Theoretical studies suggest that external electric field,[12,13] chemical functionalization or doping,[14−21] edge modification,[22−24] and defects[25,26] can alter the electronic structures of GNRs and even induce the appearance of half-metallicity (one spin channel behaves like a metal, whereas the other spin channel is a semiconductor like), which would be highly desirable in spintronics for 100% spin polarization.

However, despite of rich electronic and magnetic properties, GNRs are not mechanically robust against in-plane compression or a torsional force and a free-standing or suspending graphene is thus easily twisted or buckles, which may cause its electronic and magnetic properties to be remarkably altered.[5] Very recently, we designed a novel quasi-1D graphene nanostructure, namely, triwing graphene (TWG) nanoribbons, which not only possesses high stability, but also each wing of the TWG can retain independent electronic properties of the constituent graphene nanoribbons.[27] Moreover, zigzag-edged triwing graphene (ZZ-TWG) is a metallic ferromagnet with a large magnetic moment. Large spin polarization and high density of states were observed near the Fermi level, which suggests the ZZ-TWG could be possibly tuned to a half metal with 100% spin polarization if the Fermi level can be raised up or lowered down a little (e.g., 0.1−0.3 eV).

In this article, we presented a first-principles study on boron and nitrogen-doped (keeping the system isoelectronic) zigzag-edged triwing graphene by using BN zigzag chains replacing the carbon ones. Our results showed that BN doping can tune the ZZ-TWG from a metal into a semiconductor and even into a half-metal with considerable magnetic moments.

II. MODELS AND METHODS

The first-principles calculations were carried out using the Vienna Ab-initio Simulation Package (VASP)[28,29] by employing

Received: November 8, 2010
Revised: February 21, 2011
Published: March 23, 2011

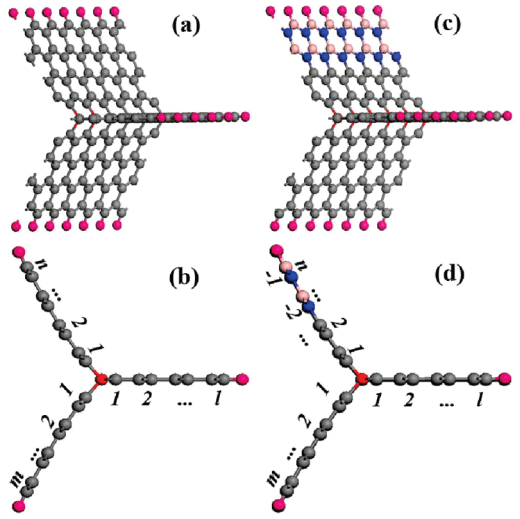

Figure 1. Structure of undoped ZZ-TWG (*n*, *m*, *l*) ((a) and (b)) and BN-doped ZZ-TWG (*n-number*, *m*, *l*) ((c) and (d)). The *n*, *m*, and *l* denote the width of three branch wings and *-number* denotes the number of BN zigzag chain. Gray, pink, dark blue and magenta balls denote carbon, boron, nitrogen and hydrogen atoms, respectively.

spin-polarized general gradient approximation (GGA) of Perdew, Burke and Ernzerhof (PBE).[30] The electron-ion interaction was described by projected augmented wave (PAW) method.[31,32] All the structures were fully optimized until the force acting on each atom was less than 0.01 eV/Å. The energy cutoff for the plane wave basis sets was 400 eV. A 1 × 1 × 35 Monkhorst−Pack k-point sampling along the 1D Brillouin zone was used.[33]

The geometric configurations of ZZ-TWG and BN-doped ZZ-TWG were shown in parts a and c of Figure 1 respectively, where the edge of each wing was passivated by hydrogen atoms. Following our previous work,[27] a ZZ-TWG constituted of three ZZ-GNRs through a sp^3 carbon-atom chain was denoted as ZZ-TWG (*n*, *m*, *l*) (part b of Figure 1), where *n*, *m*, and *l* represent the number of zigzag carbon chains in each branch ZZ-GNR wing. The doping BN zigzag chains were simply denoted by a *-number* following the number of the doped wing (part d of Figure 1), such as (*4-2*, *4*, *4*). Note that the third wing (denoted by *l*) in ZZ-TWG (*n*, *m*, *l*) is different from the other two (denoted by *n* and *m*) (part a of Figure 1) due to a C_{2v} symmetry caused by the sp^3 central carbon chain, thus (*4-2*, *4*, *4*) and (*4*, *4-2*, *4*) are equivalent doping while (*4*, *4*, *4-2*) is a different one. We adopted periodic boundary condition along the direction of ribbons.

III. RESULTS AND DISCUSSION

A. Electronic and Magnetic Properties of ZZ-TWG (*4*, *4*, *4*). H-passivated ZZ-TWGs are all metallic and ferromagnetic. We first chose ZZ-TWG (*4*, *4*, *4*) to systematically explore all the possible BN doping cases. The band structure and partial density of states (PDOS) of ZZ-TWG (*4*, *4*, *4*) were presented in part a of Figure 2. Decomposed charge density analysis reveals that three bands (labeled as **A**, **B** and **C** in part a of Figure 2) near the Fermi level are mainly contributed from the wing *n*/*m* C π orbitals, wing *l* C π^* orbitals and wing *l* C σ orbitals, respectively (part b of Figure 2). The flat band **B** is fully occupied in the spin up channel, whereas it is entirely unoccupied in the spin down channel, indicating that significant spin splitting occurs in the

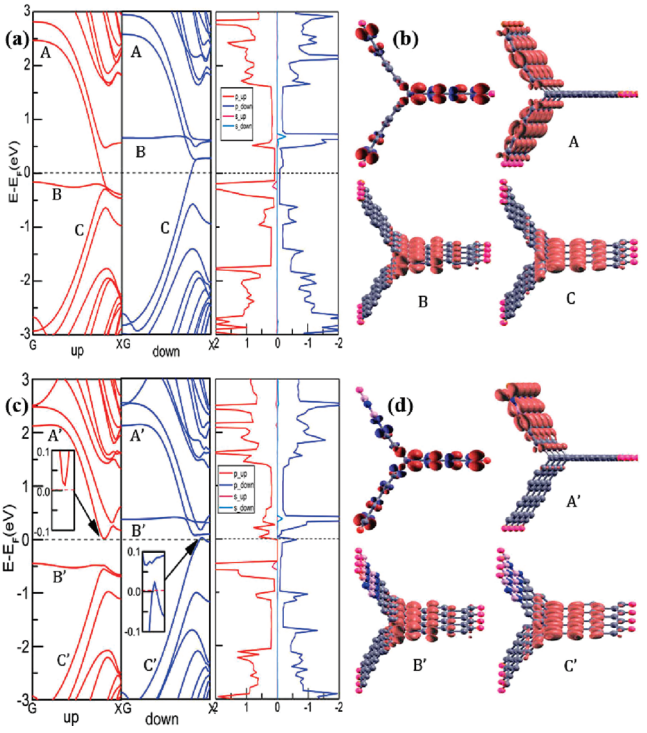

Figure 2. Band structures and PDOS of the undoped (*4*, *4*, *4*) (a) and BN-doped (*4*−*2*, *4*, *4*) (c). Spin density and decomposed charge density (isovalue =0.02 e/Å^3) of corresponding bands (labeled in (a) and (c), respectively) at Gamma point in the spin up channel (in red) for the undoped (*4*, *4*, *4*) (b) and BN-doped (*4*−*2*, *4*, *4*) (d).

wing *l* C π^* orbitals, which is responsible for the large magnetic moment of TWG. Population analysis shows that about 0.8 μ_B out of 1.5 μ_B total magnetic moment per unit of (*4*, *4*, *4*) derives from the wing *l* C atoms.

B. BN Doping in One Wing of ZZ-TWG (*4*, *4*, *4*). As shown in Figure S1 in the Supporting Information, the three branch wings of ZZ-TWGs falls into two types: the wing *l* exhibit zero DOS near the Fermi level while the wing *n*/*m* shows nonzero DOS at the Fermi level. Asymmetric doping is thus expected to induce asymmetric reconstruction in electronic structure and open the band gap. We started from one substitutional BN chain at edge of the wing *n* (or *m*) labeled as (*4-1*, *4*, *4*). The related band gap and magnetic information of the undoped and BN-doped ZZ-TWGs (4, 4, 4) are summarized in Table 1. The Fermi level is truly raised up upon BN doping while the ribbon still maintains metallicity. Interestingly, when two carbon zigzag chains at edge of the wing *n* (or *m*) are replaced by the BN ones, the doped ZZ-TWG (*4-2*, *4*, *4*) is half-metallic (part c of Figure 2) with Δ_α = 0.491 eV and Δ_β = 0 eV (Δ denotes the band gap, α and β refer to spin up and spin down channels respectively). That is, the doped ZZ-TWG (*4-2*, *4*, *4*) show conductibility for the spin-down channel whiles it is semiconducting for the spin up channel; they are thus expected to provide 100% spin-polarized current. For ZZ-TWGs are metal and BN-doped ZZ-TWGs could be half-metal, there is possibility to set up a metal/half-metal interface that is different from semiconductor/half-metal one expected in GNRs. It would be quite ideal for expected spintronics devices such as NOT gate with low power consumption in logic circuit.

To clarify the origin of half-metallicity in the doped ZZ-TWG (*4*−*2*, *4*, *4*), we computed decomposed charge density (part d of

dx.doi.org/10.1021/jp110649m |J. Phys. Chem. C 2011, 115, 6195–6199

Table 1. Δ_α, Δ_β and Magnetic Moment per Unit of (*4, 4, 4*), (*2, 2, 4*) and (*5, 5, 5*) Serial of the Undoped and BN-Doped ZZ-TWG[a]

system	Δ_α (eV)	Δ_β (eV)	electronic property	moment (μ_B)
4, 4, 4	0	0	metal	1.5
4−1, 4, 4	0	0	metal	1.4
4−2, 4, 4	0.491	0	half-metal	1.4
4−3,4, 4	0	0	metal	1.3
4−4, 4, 4	0	0	metal	1.4
4−1, 4−1, 4	0	0	metal	1.4
4−2, 4−2, 4	0.060	0	half-metal	1.4
4−3, 4−3, 4	0.402	0.249	semiconductor	1.0
4−4, 4−4, 4	1.945	1.418	semiconductor	1.0
4−4, 4−4, 4−4	1.581	1.581	semiconductor	0
2, 2, 4	0	0	metal	1.4
2−1, 2, 4	0	0.416	half-metal	1.0
2−2, 2, 4	0	0.555	half-metal	0.9
2−1, 2−1, 4	0	0	metal	0.9
2−2, 2−2, 4	0.548	2.013	semiconductor	0.9
5, 5, 5	0	0	metal	1.4
5−3, 5, 5	0	0	metal	1.3
5−4, 5, 5	0	0.393	half-metal	1.2
5−5, 5, 5	0	0.291	half-metal	0.8

[a] Δ denotes the band gap, and α and β refer to the spin up and spin down channels, respectively.

Figure 2) of the corresponding bands (labeled as **A′**, **B′** and **C′** in part c of Figure 2) near the Fermi level at Gamma point in the doped ZZ-TWG (*4*−*2*, *4*, *4*). The components of bands **B′** and **C′** remain the same as in the undoped ZZ-TWG (*4*, *4*, *4*). However, the band **A′** is mainly contributed from the B and N π orbitals which are completely unoccupied and localized at the doped wing ***n*** of doped ZZ-TWG (*4*−*2*, *4*, *4*). In contrast, the band **A** from the C π orbitals is partially occupied and locates at wings ***n*** and ***m*** of the undoped ZZ-TWG (*4*, *4*, *4*). Meanwhile, the spin splitting of band **A** of the undoped ZZ-TWGs is considerably released in the BN-doped ZZ-TWGs and the magnetism of ZZ-TWGs is thus reduced (Table 1). We also found that the spin polarization of the doped wing is nearly completely suppressed (part d of Figure 2), whereas the undoped wings are less affected. This is consistent with the independence of each wing revealed in our previous work.[27] Such spin polarization suppression behavior is also observed in nitrogen doping,[15] boron doping and vacancies[34] in ZZ-GNRs. We supposed that, together with intrinsic magnetism, such a spin polarization asymmetric distribution caused by asymmetric BN doping is responsible for driving up Fermi level and opening band gap, and is an essential factor in giving rise to the observed half-metallic behavior.

C. BN Doping in Two Wings of ZZ-TWG (*4, 4, 4*). Compared with asymmetric doping, symmetric BN doping in ZZ-TWG is more difficult to achieve from the energy point of view, for example, (*4*−*1*, *4*−*1*, *4*) is 1.03 eV higher in energy than (*4*−*2*, *4*, *4*). With two BN chains doped at the end of the wings ***n*** and ***m***, the doped ZZ-TWG (*4-2*, *4-2*, *4*) (part a of Figure 3) exhibits a poor half-metallicity with a very small Δ_α (0.060 eV). This suggests symmetric BN doping simultaneously suppresses the spin polarization in both wings and cannot open an obvious band gap in any spin channel, leading to the weak half-metallicity in (*4-2*, *4-2*, *4*). However, when these two doped BN chains move

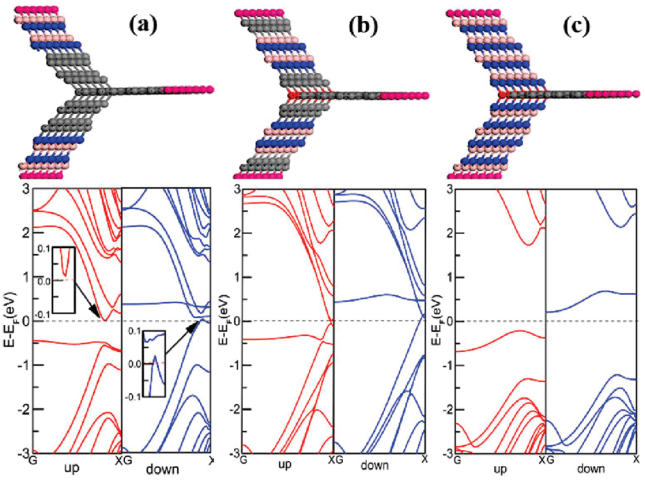

Figure 3. Geometries and band structures of the BN-doped ZZ-TWG (*4*−*2*, *4*−*2*, *4*) (a), and its isomer of (*4*−*2*, *4*−*2*, *4*) (b), and (*4*−*4*, *4*−*4*, *4*) (c).

toward the central, (*4-2*, *4-2*, *4*) (part b of Figure 3) shows fully metallicity in both channels. This is because such doping neither breaks the edge states which govern the electronic properties of ZZ-TWG nor suppresses the localized spin polarization of corresponding wings and thus such a doped ZZ-TWG shows metallicity like an undoped ZZ-TWG. This implies that the BN doping site is also an important factor in tuning the electronic properties of ZZ-TWGs.

Moreover, we found that heavily symmetric doping in ZZ-TWG (*4, 4, 4*) can even turn a metal ZZ-TWG into a semiconductor with Δ_α = 1.945 eV and Δ_β = 1.417 eV (indirect gap =0.230 eV), respectively (part c of Figure 3). Such a doped ZZ-TWG (*4*−*4*, *4*−*4*, *4*) can be regarded as two zigzag boron nitrogen nanoribbons (ZZ-BNNR) combined with a ZZ-GNR by a sp^3 carbon chain or an 8-ZZ-BNNR been inserted by a 4-ZZ-GNR. Here, we found that with increasing doping concentration along with proper doping site the BN-doped ZZ-TWG shows a metal−half-metal−semiconductor transition. We also considered an extreme case that all carbon chains of three wings are replaced by BN ones, namely zigzag-edged triwing BN nanoribbon (*4*−*4*, *4*−*4*, *4*−*4*) and found it is a nonmagnetic semiconductor with spin polarization entirely been suppressed.

To evaluate the relative stability of BN-doped TWG, we computed the formation energies of the BN-doped TWG(4, 4, 4) under different BN doping concentration. The formation energy (FE) is defined as follows:

$$\mathrm{FE} = [E(\mathrm{BN-TWG}) - N_C E_C - N_H E_H - N_N E_N - N_B E_B] - \mathrm{FE}(\mathrm{wing}\ \boldsymbol{n}) - \mathrm{FE}(\mathrm{wing}\ \boldsymbol{m}) - \mathrm{FE}(\mathrm{wing}\ \boldsymbol{l})$$

$$\mathrm{FE}(\mathrm{wing}\ \boldsymbol{x}, \boldsymbol{x} = \boldsymbol{n}, \boldsymbol{m}, \boldsymbol{l}) = [\mathrm{E}(\mathrm{wing}\ \boldsymbol{x}) - N_C E_C - N_H E_H - N_N E_N - N_B E_B]/2$$

Where N_C, N_H, N_N, and N_B are the number of carbon, hydrogen, nitrogen and boron atoms per unit cell in the corresponding systems, E_C, E_H, E_N, and E_B are the energy of perfect graphene, hydrogen molecule, nitrogen molecule, and α-rhombohedral boron per atom, respectively. E(BN-TWG) and E(wing ***x***) are the total energy per unit cell of BN-doped TWG and wing ***x*** (***x*** = ***n***, ***m***, ***l***) systems, and the FE(wing ***x***) is the formation energy per unit cell

dx.doi.org/10.1021/jp110649m |*J. Phys. Chem. C* 2011, 115, 6195–6199

Table 2. Formation Energies of Asymmetric (Left Half) BN-Doped and Symmetric (Right Half) Doped (*4, 4, 4*) Serials ZZ-TWG

structures	formation energy (eV)	structures	formation energy (eV)
4−1, 4, 4	−1.46	4−1, 4−1, 4	−0.91
4−2, 4, 4	−1.41	4−2, 4−2, 4	−0.83
4−3, 4, 4	−1.43	4−3, 4−3, 4	−1.02
4−4, 4, 4	−1.50	4−4, 4−4, 4	−1.31

of wing ***x***. The formation energies of all the BN-doped TWG(4,4,4) are all negative as shown in Table 2. This indicates that the formation processes are all exothermic, which means the feasibility of making BN-doped TWG. Similar to our proposed pure TWG nanoribbons, such a BN-doped triwing graphene can be fabricated by fusing a GNR edge vertically to a flat BN-doped GNR. The BN-doped GNRs can be synthesized from a hybridized boron nitride and graphene domains[35] or from unzipping of B−C−N single-walled nanotubes.[36]

D. BN Doping in ZZ-TWG (*2, 2, 4*). Above, we investigated ***n*** = ***m*** = ***l*** type ZZ-TWGs (***n, m, l***) with BN doping. For the wing ***n***/***m*** showing metallic behavior while wing ***l*** behaving like a semiconductor in ZZ-TWG (also part a of Figure S1 of the Supporting Information), we also considered ***n*** = ***m*** < ***l*** type ZZ-TWGs with two narrow wings, of which BN doping is expected to break the edge states and suppress the spin polarization much easily. We chose (*2, 2, 4*) as an example for comparison which it is expected to show distinct doping effect. Moreover, the edges of wings ***n*** and ***m*** in (*2, 2, 4*) are very close to the sp^3 central carbon axis that can be viewed as a special common edge of three wings, and doping at edges of the wings ***n*** and/or ***m*** will affect the edge of other wing(s), which may also bring some different influence to the electronic structure of the TWGs. Asymmetrically doped ZZ-TWG (*2-1, 2, 4*) with one BN chain substitution and (*2-2, 2, 4*) with two BN chains substitutions were taken into account. Their band structures were displayed in parts and b of Figure 4, respectively. As clearly seen from the figures, the (*2-1, 2, 4*) and (*2-2, 2, 4*) are both robust half-metals: (*2-1, 2, 4*) with Δ_β = 0.416 eV and (*2-2, 2, 4*) with Δ_β = 0.555 eV, respectively. However, the symmetric doping (*2-1, 2−1, 4*), an isomer of (*2-2, 2, 4*) is still metallic. Meanwhile, the heavily doping as (*2-2, 2-2, 4*) in ZZ-TWG (*2, 2, 4*) also turns it from a metal into a semiconductor. These results support our earlier argument that asymmetric spin polarization distribution caused by asymmetric BN doping can lead to fruitful electronic properties even half-metallicity, and such asymmetric doping becomes a very important factor in engineering electronic structures of the ribbons.

E. (*5, 5, 5*) Serial Asymmetric BN-Doped ZZ-TWG. To find out whether the branch ribbons widths correlate with the doping effect, we also studied the electronic properties of (*5, 5, 5*) serial BN-doped ZZ-TWG and the results are included in Table 1. Similar to the case of (*4, 4, 4*), with the increase of the BN doping concentration, ZZ-TWG (*5, 5, 5*) serials can be tuned from a metal into a half-metal ((*5-4, 5, 5*) and (*5-5, 5, 5*)) and the magnetic moments are gradually decreased. Different from the case of (*4, 4, 4*), to achieve the half-metallicity, more BN zigzag chains are needed in (*5, 5, 5*) serial BN-doped ZZ-TWG. This suggests that a critical ratio of BN to C should be satisfied to the presence of the half-metallicity. Asymmetric doping in proper position and an appropriate BN to C ratio would be the key factors to realize half-metallicity in this system.

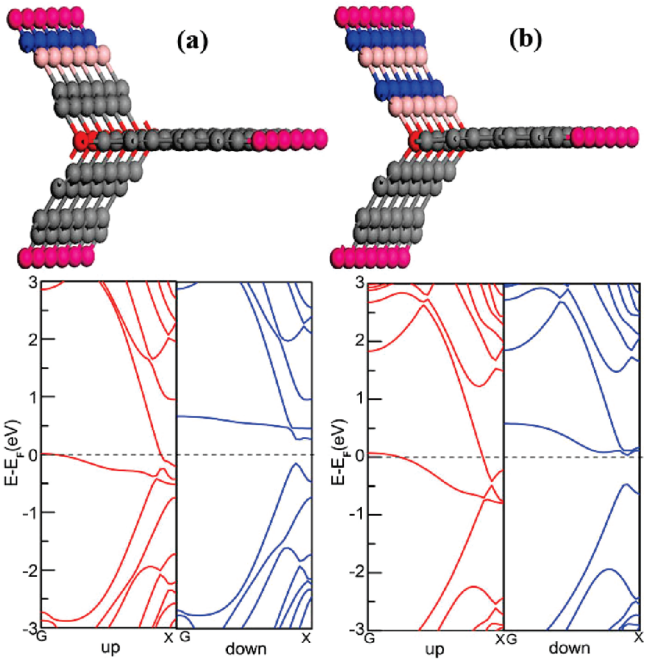

Figure 4. Geometries and band structures of BN-doped ZZ-TWG: (a) (*2−1, 2, 4*) and (b) (*2−2, 2, 4*).

IV. CONCLUSIONS

In summary, the electronic properties of (*4, 4, 4*), (*2, 2, 4*), and (*5, 5, 5*) serial BN-doped ZZ-TWG nanoribbons have been investigated within the framework of spin polarized density functional theory. The asymmetric doping (*4−2, 4, 4*) with two BN zigzag chains substitution on one wing of (*4, 4, 4*) suppresses the spin polarization of the doped wing and turns the TWG into a half-metal, while the symmetric BN doping or nonedged asymmetric BN doping retains the metallic nature or induces poor half-metallicity with a very small half-metal gap. The asymmetric BN doping gives rise to more robust half-metallicity in (*2, 2, 4*) serial and in (*5, 5, 5*) serial doped ZZ-TWGs. Whereas heavily doping can turn a metallic ZZ-TWG into a semiconductor. These results suggest that asymmetric BN doping is an essential origin of the observed half-metallicity, as well as the proper doping site and the BN doping concentration, which helps us to design good half-metallic nanostructures for spintronics devices.

Finally, we would like to clarify the influences of the lattice mismatch (1.3%) between the BN nanosheet and graphene nanosheet, which may induce out-of-plane rippling and warping if a finite length of the doped ribbons is used. We calculated the undoped (*4, 4, 4*) and BN-doped (*4−2, 4, 4*) ZZ-TWG with a finite length (5 cycles along ribbon direction, about 1.31 nm). We do not observe obvious out-of-plane deformation in the undoped and BN-doped ZZ-TWG, and the electronic and magnetic properties do not change much either. These results confirm again that the triwing structures we proposed before are mechanically robust to against the in-plane compression or torsional force.

■ ASSOCIATED CONTENT

Supporting Information. Figure of local densities of states (LDOS) of undoped ZZ-TWG (*4, 4, 4*) and of doped

ZZ-TWG (*4*−*2*, *4*, *4*); figure of optimized structures of undoped ZZ-TWG (*4*, *4*, *4*) and BN-doped ZZ-TWG (*4*−*2*, *4*, *4*) with finite lengths. This material is available free of charge via the Internet at http://pubs.acs.org.

AUTHOR INFORMATION

Corresponding Author
*E-mail: jlwang@seu.edu.cn.

ACKNOWLEDGMENT

This work is supported by the NSF (11074035, 20873019), NBRP (2010CB923401, 2011CB302004, 2009CB623200), SRFDP (20090092110025), the Outstanding Young Faculty Grant, and Peiyu Foundation of SEU in China. The authors thank the computational resource at Department of Physics, SEU.

REFERENCES

(1) Novoselov, K. S.; Geim, A. K.; Morozov, S. V.; Jiang, D.; Zhang, Y.; Dubonos, S. V.; Grigorieva, I. V.; Firsov, A. A. *Science* **2004**, *306*, 666–669.
(2) Berger, C.; Song, Z. M.; Li, X. B.; Wu, X. S.; Brown, N.; Naud, C.; Mayou, D.; Li, T. B.; Hass, J.; Marchenkov, A. N.; Conrad, E. H.; First, P. N.; de Heer, W. A. *Science* **2006**, *312*, 1191–1196.
(3) Katsnelson, M. I. *Mater. Tod.* **2007**, *10*, 20–27.
(4) Trauzettel, B.; Bulaev, D. V.; Loss, D.; Burkard, G. *Nat. Phys.* **2007**, *3*, 192–196.
(5) Neto, A. H. C.; Guinea, F.; Peres, N. M. R.; Novoselov, K. S.; Geim, A. K. *Rev. Mod. Phys.* **2009**, *81*, 109–162.
(6) Allen, M. J.; Tung, V. C.; Kaner, R. B. *Chem. Rev.* **2010**, *110*, 132–145.
(7) Son, Y. −W.; Cohen, M. L.; Louie, S. G. *Phys. Rev. Lett.* **2006**, *97*, 216803.
(8) Barone, V.; Hod, O.; Scuseria, G. E. *Nano Lett.* **2006**, *6*, 2748–2574.
(9) Li, X. L.; Wang, X. R.; Zhang, L.; Lee, S.; Dai, H. J. *Science* **2008**, *319*, 1229–1232.
(10) Ritter, K. A.; Lyding, J. W. *Nat. Mater.* **2009**, *8*, 235–242.
(11) Pisani, L.; Chan, J. A.; Montanari, B.; Harrison, N. M. *Phys. Rev. B* **2007**, *75*, 064418.
(12) Son, Y. −W.; Cohen, M. L.; Louie, S. G. *Nature* **2006**, *444*, 347–349.
(13) Zhang, Y. B.; Tang, T. −T.; Girit, C.; Hao, Z.; Martin, M. C.; Zettl, A.; Crommie, M. F.; Shen, Y. R.; Wang, F. *Nature* **2009**, *459*, 820–823.
(14) Nduwimana, A.; Wang, X. Q. *ACS Nano* **2009**, *3*, 1995–1999.
(15) Li, Y. F.; Zhou, Z.; Shen, P. W.; Chen, Z. F. *ACS Nano* **2009**, *3*, 1952–1958.
(16) Cervantes-Sodi, F.; Csányi, G.; Piscanec, S.; Ferrari, A. C. *Phys. Rev. B* **2008**, *77*, 165427.
(17) Martins, T. B.; Miwa, R. H.; da Silva, A. J. R.; Fazzio, A. *Phys. Rev. Lett.* **2007**, *98*, 196803.
(18) Dutta, S.; Manna, A. K.; Pati, S. K. *Phys. Rev. Lett.* **2009**, *102*, 096601.
(19) Kan, E. -J.; Wu, X. J.; Li, Z. Y.; Zeng, X. C.; Yang, J. L.; Hou, J. G. *J. Chem. Phys.* **2008**, *129*, 084712.
(20) Gorjizadeh, N.; Farajian, A. A.; Esfarjani, K.; Kawazoe, Y. *Phys. Rev. B* **2008**, *78*, 155427.
(21) Dutta, S.; Lakshmi, S.; Pati, S. K. *Phys. Rev. B* **2008**, *77*, 073412.
(22) Kan, E. −J.; Li, Z. Y.; Yang, J. L.; Hou, J. G. *J. Am. Chem. Soc.* **2008**, *130*, 4224–4225.
(23) Kudin, K. N. *ACS Nano* **2008**, *2*, 516–522.
(24) Hod, O.; Barone, V.; Peralta, J. E.; Scuseria, G. E. *Nano Lett.* **2007**, *7*, 2295–2299.
(25) Martins, T. B.; da Silva, A. J. R.; Miwa, R. H.; Fazzio, A. *Nano Lett.* **2008**, *8*, 2293–2298.
(26) Dutta, S.; Pati, S. K. *J. Phys. Chem. B* **2008**, *112*, 1333–1335.
(27) Zhu, L. Y.; Wang, J. L.; Zhang, T. T; Ma, L.; Lim, C. W.; Ding, F.; Zeng, X. C. *Nano Lett.* **2010**, *10*, 494–498.
(28) Kresse, G.; Hafner, J. *Phys. Rev. B* **1993**, *48*, 13115–13118.
(29) Kresse, G.; Furthmüller, J. *Comput. Mater. Sci.* **1996**, *6*, 15–50.
(30) Perdew, J. P.; Burke, K.; Ernzerhof, M. *Phys. Rev. Lett.* **1996**, *77*, 3865–3868.
(31) Blöchl, P. E. *Phys. Rev. B* **1994**, *50*, 17953–17979.
(32) Kresse, G.; Joubert, D. *Phys. Rev. B* **1999**, *59*, 1758–1775.
(33) Monkhorst, H. J.; Pack, J. D. *Phys. Rev. B* **1976**, *13*, 5188–5192.
(34) Huang, B.; Liu, F.; Wu, J.; Gu, B. −L.; Duan, W. H. *Phys. Rev. B* **2008**, *77*, 153411.
(35) Ci, L.; Song, L.; Jin, C. H.; Jariwala, D.; Wu, D. X.; Li, Y. J.; Srivastava, A.; Wang, Z. F.; Storr, K.; Balicas, L.; Liu, F.; Ajayan, P. M. *Nat. Mater.* **2010**, *9*, 430–435.
(36) Wang, W. L.; Bai, X. D.; Liu, K. H.; Xu, Z.; Golberg, D.; Bando, Y.; Wang, E. G. *J. Am. Chem. Soc.* **2006**, *128*, 6530–6531.